



Brief communication: The anomalous winter 2019 sea ice conditions in McMurdo Sound, Antarctica

Greg H. Leonard¹, Kate E. Turner^{2, 3}, Maren E. Richter², Maddy S. Whittaker², and Inga J. Smith²

¹National School of Surveying, University of Otago, Dunedin, New Zealand

²Department of Physics, University of Otago, Dunedin, New Zealand

³National Institute of Water and Atmospheric Research, Wellington, New Zealand

Correspondence: Greg Leonard (greg.leonard@otago.ac.nz)

Abstract.

McMurdo Sound sea ice can generally be partitioned into two regimes: (1) a stable fast-ice cover, forming south of approximately 77.6° S around March / April, then breaking out the following January / February; and, (2) a more dynamic region north of 77.6° S that the McMurdo Sound and Ross Sea polynyas regularly impact. In 2019, a stable fast-ice cover formed unusually late due to repeated break-out events. We analyse the 2019 sea-ice conditions and relate them to southerly wind events using a Katabatic Wind Index (KWI). We find there is a strong correlation between break-out events and several unusually large KWI events.

1 Introduction

The sea-ice cover in McMurdo Sound can generally be partitioned into two regimes: (1) a stable fast-ice cover occupying the southeastern and western parts of the Sound, south of a latitude of approximately 77.6° S; and, (2) a more dynamic region in the central part of the Sound. Regime (1) is primarily made up of first-year sea ice that forms around late March / early April and typically breaks out in January / February of the following year (Kim et al., 2018) whereas Regime (2) is impacted by the McMurdo Sound Polynya (MSP) and Ross Sea Polynya (RSP) (Brett et al.). The boundary between the regimes is influenced by such factors as ice-shelf ocean interactions, ocean circulation (e.g. Hughes et al., 2014; Robinson et al., 2014) and the location of grounded icebergs (e.g. Brunt et al., 2006; Robinson and Williams, 2012) and can vary on annual timescales.

McMurdo Sound logistical and scientific sea ice operations depend on the formation of a stable fast-ice cover over the winter months that persists through to late December / early January. In 2019, the formation of the fast ice cover was significantly delayed, impacting operations for both the New Zealand and the United States of America Antarctic programmes. Impacts included: the non-establishment of a sea ice route to Marble Point (a cache for helicopter fuel and other supplies); a reduction in the number of sea ice scientific field sites; and a two-month delay in the deployment of the University of Otago sea ice mass balance station.



We are not aware of any studies directly investigating the causes of delayed freeze-up of sea ice in McMurdo Sound. Kim et al. (2018) found that in years with higher mean annual wind speeds, the fast ice generally retreated earlier in the season, however, that study did not look at the impact of individual events on break up and retreat. At the event level, investigations by Banwell et al. (2017) into causes of the calving of the McMurdo Ice Shelf in 2016 suggested that strong ($>10 \text{ m s}^{-1}$) winds from the south and west contributed to the large fast ice break-up event that preceded the calving event. Brunt et al. (2006) investigated sea-ice break-out events in the southwest Ross Sea between 1996 and 2005 using satellite imagery and automatic weather station data. They found that break-out events were correlated with a dimensionless “storm index”, defined as the product of low pressure anomalies and anomalous temperature (lower temperatures in summer and higher temperatures in winter).

In this brief communication we investigate the linkages between enhanced MSP activity, due to increased winter storm frequency and intensity, and the delay in the formation of a stable fast ice cover in 2019. We quantify winter storm intensity by introducing a Katabatic Wind Index (KWI) that is based on the approach of Brunt et al. (2006), but here is applied to individual events as opposed to seasonal trends. 2019 McMurdo Sound sea ice cover properties are derived from a combination of manual assessment of Synthetic Aperture Radar (SAR) and MODIS derived ice surface temperatures and analysing sea ice concentrations generated by the ARTIST Sea Ice (ASI) algorithm (Spren et al., 2008).

2 McMurdo Sound sea ice characteristics

The edge of the stable fast-ice cover typically extends west-to-east from a band of fast ice $\sim 20 \text{ km}$ wide along the Victoria Land Coast to Cape Royds, Ross Island (see Figure 1a). To investigate when this sea ice cover forms, we analysed the Fraser et al. (2020) circum-Antarctic land-fast sea-ice distribution data set derived from cloud-free, 14-day composites of satellite visible–thermal infrared imagery. This data set covers the period from March 2000 to February 2018 and includes the time period when the sea ice in McMurdo Sound was strongly impacted by the presence of very large, tabular icebergs (e.g. C-19 and B-15A) at the mouth of the Sound.

From 2001 to 2005, the sea ice (Brunt et al., 2006) and ocean circulation (Robinson and Williams, 2012) in McMurdo Sound were directly influenced by these icebergs, leading to the presence of multi-year ice and anomalously large sea ice extents that biased the studies of Brunt et al. (2006) and Kim et al. (2018). The effects on the fast ice in McMurdo Sound were felt for several years after the icebergs exited the region, as evidenced by the fact that a multi-year fast ice covered remained in place in the southern part of the Sound until February 2011. Therefore, the fast ice extents for these years (2001 – 2011) have been excluded from our analysis.

In years that were not iceberg-affected (2000; 2012 – 2017), the fast ice cover in the Sound generally reached a minimum in mid-March where it typically recedes into a few pockets along the Victoria Land Coast in the west of the Sound, around the Erebus Glacier Tongue along the west coast of Ross Island and into a wedge-shaped area between the tip of the Hut Point Peninsula on Ross Island and the McMurdo Ice Shelf. The fast ice cover south of 77.6° S typically re-forms sometime between



55 mid-March and mid-April, with the exception of 2012, where it did not form until around the end of June. This is contrasted
 with 2019 when a stable fast-ice cover did not form until late July.

2.1 2019 sea ice conditions

An analysis of radar (Sentinel-1 SAR) imagery and MODIS 1 km resolution ice surface temperatures (Hall and Riggs, a, b) during the period April – July 2019 revealed an unusually large number of MSP events, and the frequency and intensity of
 60 these events impacted the fast-ice cover by repeatedly eroding it all the way back to the edge of the ice shelf, which is ~30 km farther south than 77.6° S. Prior to the events, MODIS ice surface temperatures typically showed warming in the east of the Sound, suggesting a fractional ice cover and removal of first-year ice, consistent with activation of the MSP. From 15 April to 1 September, eight large MSP events were observed in SAR images, including 21 May, 25 June and 8 July (reference Figure 1b – d) and 19 and 21 April, 6 and 8 May and 10 June (not shown).

65 Manually identified events were contextualised with sea ice concentrations derived from the ARTIST Sea Ice (ASI) algorithm (Spreen et al., 2008). Figure 1e and f show sea ice concentrations for the late-June and mid-July event, respectively. The ARTIST landmask extends up to ~15 km into the southern Sound, hence sea ice concentrations cannot be determined in this area. In comparing Figure 1c to Figure 1e it can be seen that the late-June event broke up the fast ice cover all the way back to the edge of the ice shelf, but this has not been fully captured in the ARTIST sea ice concentration due to the land mask. This
 70 delayed the impact of the late-June event on the ARTIST sea ice concentrations by a couple of days, which will be discussed further in Section 4.

3 Characterisation of winter storms

Strong wind events in this region are dominated by southerly katabatic and barrier winds that flow off the Ross Ice Shelf (e.g. Coggins et al., 2013; Parish et al., 2006) and are channeled into McMurdo Sound. These winds are typically connected to warm
 75 temperatures and low air pressure (e.g. Coggins et al., 2013; Chenoli et al., 2013). During winter, higher wind speeds (above 4 – 6 m s⁻¹) increase the mixing between the cold surface inversion layer over the ice shelf and the warmer overlying atmosphere (Cassano et al., 2016). The increase in temperature may also be partly influenced by the Föhn effect, whereby katabatic winds from the Transantarctic Mountains, one of the sources of southerly winds on the Ross Ice Shelf (Parish et al., 2006), experience adiabatic warming. Southerly wind events in the Ross Sea are correlated to sea ice concentration and the opening of the Ross
 80 Sea Polynya (RSP) (Dale et al., 2017) and in the following we will examine this relationship for the McMurdo Sound Polynya in 2019.

The wind climatologies for Scott Base (Figure 2) show that the months leading to the freeze-up of McMurdo Sound in 2019 were characterised particularly strong southerly winds. To investigate this further, following the approach of Brunt et al. (2006), we used hourly 20 m air temperature and atmospheric pressure data from the Scott Base weather station to construct
 85 a dimensionless Katabatic Wind Index (KWI). As the period of interest spans only the winter months, we define the KWI as the product of the positive air temperature and negative mean sea level pressure anomalies, as calculated in relation to the



climatological mean. This index was then smoothed over a 12-hour window. The index, and the corresponding air temperature and mean sea level pressure data, are shown in Figure 3.

As defined by this index, in the period 15 April to 1 September, three large katabatic wind events leading to MSP activations occurred in mid-June, late-June and mid-July of 2019, coincident with times when large break-out events were identified. Two smaller events occurred in May. There were also several KWI events in August that did not lead to large break-out events.

4 Impact of mid-winter southerly wind events on the 2019 fast ice cover

To quantify the effect of katabatic events on the 2019 sea ice cover, we first computed a daily sea ice fraction for McMurdo Sound for the period 15 April to 1 September over the entire ARTIST record (2013 – 2019). The sea ice fraction was calculated by summing the number of pixels within the bounds of the red box shown in Figure 1a where the sea ice concentration was 15 % or greater and dividing by the total number of pixels ($n = 553$), excluding land masked pixels.

The sea ice fractions for the years 2013 – 2019 are shown in Figure 3a, with the 2019 data indicated by a thick black line. It can be clearly seen that the timing of low (< 0.8) sea ice fraction events correspond with identified sea ice break-out events, even though the sea ice fraction is likely underestimating the amount of open water due to the protrusion of the ARTIST land mask into the southern reaches of the Sound. An example of this is the late-June event (reference Figure 1c) where the sea ice fraction decrease lags the KWI and the manually identified break-out event by a couple of days. This break-out event was characterised by the MSP first activating just off the edge of the ice shelf (which is masked out in the ARTIST sea ice concentrations) before expanding northward, whereas in other events the polynya tends to be centred farther to the North. The 2019 record stands apart from other years in terms of the number of low ice fraction events overall, and particularly during the months of June and July where it was the only year in the time series to record low sea ice fraction events during these months.

5 Conclusions

Our analysis implies that the stability of the McMurdo Sound fast-ice cover south of 77.6° S is potentially vulnerable to storm events from late spring to mid-winter. The fast-ice cover tends to be more responsive to storm events in April and May, presumably because the ice cover is still relatively thin and warm and lacks the strength to resist the drag force from the southerly winds. The KWI climatology indicates that the frequency and intensity of southerly storms tends to decrease in the months of June and July. This typically allows the fast ice cover to thicken and gain strength during these months, which means that it is sufficiently strong to remain intact when the southerly winds increase, on average, later in the year.

In 2019, the frequency and intensity of storms in June and July were such that the fast-ice cover was too weak to withstand the southerly winds and was broken up and advected northwards on three separate occasions. Immediately following the mid-July event, the KWI indicates a more quiescent weather pattern, allowing the fast ice cover to reform and gain strength. The KWI increases again in mid-August, however, the fast-ice cover south of 77.6° S is now able to resist the southerly wind stress



and stays fixed in place for the remainder of the growth season. This result is generally consistent with the findings of Brett et al. who described the impact of increased southerly winds in winter in 2011 and 2017 on McMurdo Sound fast ice.

120 *Data availability.* Scott Base weather station data is available from <https://cliflo.niwa.co.nz/> and Linda AWS data is available through <https://amrc.ssec.wisc.edu/aws/>, Lazzara et al. (2012). Sentinel-1 SAR images were accessed through the Alaska Satellite Facility DAAC, at <https://search.asf.alaska.edu/> and MODIS images were accessed through <https://urs.earthdata.nasa.gov>. ARTIST sea ice concentration data accessed from the University of Bremen data archive at <https://seaice.uni-bremen.de/data/>.

Author contributions. GHJ had the initial idea for this study and analysed the satellite images and Fraser et al. (2020) and Spreen et al. (2008) data sets. KET analysed the climatological data in reference to the break out events and designed the KWI. MER analysed the Scott
125 Base weather station climatology. MSW identified break out events in 2019 from SAR and MODIS images. GHJ, KET, MER and IJS discussed the results and prepared the manuscript. All authors contributed to the final review of the manuscript.

Competing interests. There are no competing interests.

Acknowledgements. This paper is an output from the project "Supercooling measurements under ice shelves" supported by the Marsden Fund Council from Government funding, administered by the Royal Society of New Zealand (Marsden Fund contract number MFP-UOO1825).
130 MSW was supported on a summer scholarship from that project, and IJS and GHJ's time was supported by that project. MER is supported by a University of Otago Doctoral Scholarship and an Antarctica New Zealand Sir Robin Irvine Post-Graduate Scholarship.



References

- Banwell, A. F., Willis, I. C., Macdonald, G. J., Goodsell, B., Mayer, D. P., Powell, A., and Macayeal, D. R.: Calving and rifting on the
 McMurdo Ice Shelf, Antarctica, *Annals of Glaciology*, 58, 78–87, <https://doi.org/10.1017/aog.2017.12>, 2017.
- 135 Brett, G. M., Irvin, A., Rack, W., Haas, C., Langhorne, P. J., and Leonard, G. H.: Variability in the Distribution of Fast Ice
 and the Sub-ice Platelet Layer Near McMurdo Ice Shelf, *Journal of Geophysical Research: Oceans*, 125, e2019JC015678,
<https://doi.org/10.1029/2019JC015678>.
- Brunt, K. M., Sergienko, O., and MacAyeal, D. R.: Observations of unusual fast-ice conditions in the southwest Ross Sea, Antarctica:
 preliminary analysis of iceberg and storminess effects, *Annals of Glaciology*, 44, 183–187, <https://doi.org/10.3189/172756406781811754>,
 140 2006.
- Cassano, J. J., Nigro, M. A., and Lazzara, M. A.: Characteristics of the near-surface atmosphere over the Ross Ice Shelf, Antarctica, *Journal*
of Geophysical Research: Atmospheres, 121, 3339–3362, <https://doi.org/10.1002/2015JD024383>, 2016.
- Chenoli, S. N., Turner, J., and Samah, A. A.: A climatology of strong wind events at McMurdo station, Antarctica, *International journal of*
climatology, 33, 2667–2681, <https://doi.org/10.1002/joc.3617>, 2013.
- 145 Coggins, J. H. J., McDonald, A., and Jolly, B.: Synoptic climatology of the Ross Ice Shelf and Ross Sea region of Antarctica: *k*-means
 clustering and validation, *International Journal of Climatology*, 34, 2330–2348, <https://doi.org/10.1002/joc.3842>, 2013.
- Dale, E. R., McDonald, A. J., Coggins, J. H. J., and Rack, W.: Atmospheric forcing of sea ice anomalies in the Ross Sea polynya region.,
The Cryosphere, 11, 267–280, <https://doi.org/10.5194/tc-11-267-2017>, 2017.
- Fraser, A. D., Massom, R. A., Ohshima, K. I., Willmes, S., Kappes, P. J., Cartwright, J., and Porter-Smith, R.: High-resolution mapping of
 150 circum-Antarctic landfast sea ice distribution, 2000–2018, *Earth System Science Data Discussions*, 12, 1–18, <https://doi.org/10.5194/essd-12-2987-2020>, 2020.
- Hall, D. K. and Riggs, G. A.: MODIS/Aqua Sea Ice Extent 5-Min L2 Swath 1km, Version 6. [Ice Temperature]. Boulder, Colorado USA.
 NASA National Snow and Ice Data Center Distributed Active Archive Center., <https://doi.org/10.5067/MODIS/MYD29.006>, a.
- Hall, D. K. and Riggs, G. A.: MODIS/Terra Sea Ice Extent 5-Min L2 Swath 1km, Version 6. [Ice Temperature]. Boulder, Colorado USA.
 155 NASA National Snow and Ice Data Center Distributed Active Archive Center., <https://doi.org/10.5067/MODIS/MYD29.006>, b.
- Hughes, K. G., Langhorne, P. J., Leonard, G. H., and Stevens, C. L.: Extension of an Ice Shelf Water plume model beneath sea ice with appli-
 cation in McMurdo Sound, Antarctica, *Journal of Geophysical Research: Oceans*, 119, 8662–8687, <https://doi.org/10.1002/2013jc009411>,
 2014.
- Kim, S., Saenz, B., Scanniello, J., Daly, K., and Ainley, D.: Local climatology of fast ice in McMurdo Sound, Antarctica, *Antarctic Science*,
 160 30, 125–142, <https://doi.org/10.1017/s0954102017000578>, 2018.
- Lazzara, M. A., Weidner, G. A., Keller, L. M., Thom, J. E., and Cassano, J. J.: Antarctic automatic weather station program: 30 years of polar
 observations, *Bulletin of the American Meteorological Society*, 93, 1519–1537, <https://doi.org/10.1175/BAMS-D-11-00015.1>, 2012.
- Parish, T. R., Cassano, J. J., and Seefeldt, M. W.: Characteristics of the Ross Ice Shelf air stream as depicted in Antarctic Mesoscale Prediction
 System simulations, *Journal of Geophysical Research: Atmospheres*, 111, <https://doi.org/10.1029/2005JD006185>, 2006.
- 165 Robinson, N. J. and Williams, M. J. M.: Iceberg-induced changes to polynya operation and regional oceanography in the southern Ross Sea,
 Antarctica, from in situ observations, *Antarctic Science*, 24, 514–526, <https://doi.org/10.1017/s0954102012000296>, 2012.



- Robinson, N. J., Williams, M. J. M., Stevens, C. L., Langhorne, P. J., and Haskell, T. G.: Evolution of a supercooled Ice Shelf Water plume with an actively growing subice platelet matrix, *Journal of Geophysical Research: Oceans*, 119, 3425–3446, <https://doi.org/10.1002/2013JC009399>, 2014.
- 170 Spreen, G., Kaleschke, L., and Heygster, G.: Sea ice remote sensing using AMSR-E 89-GHz channels, *Journal of Geophysical Research: Oceans*, 113, <https://doi.org/10.1029/2005JC003384>, 2008.

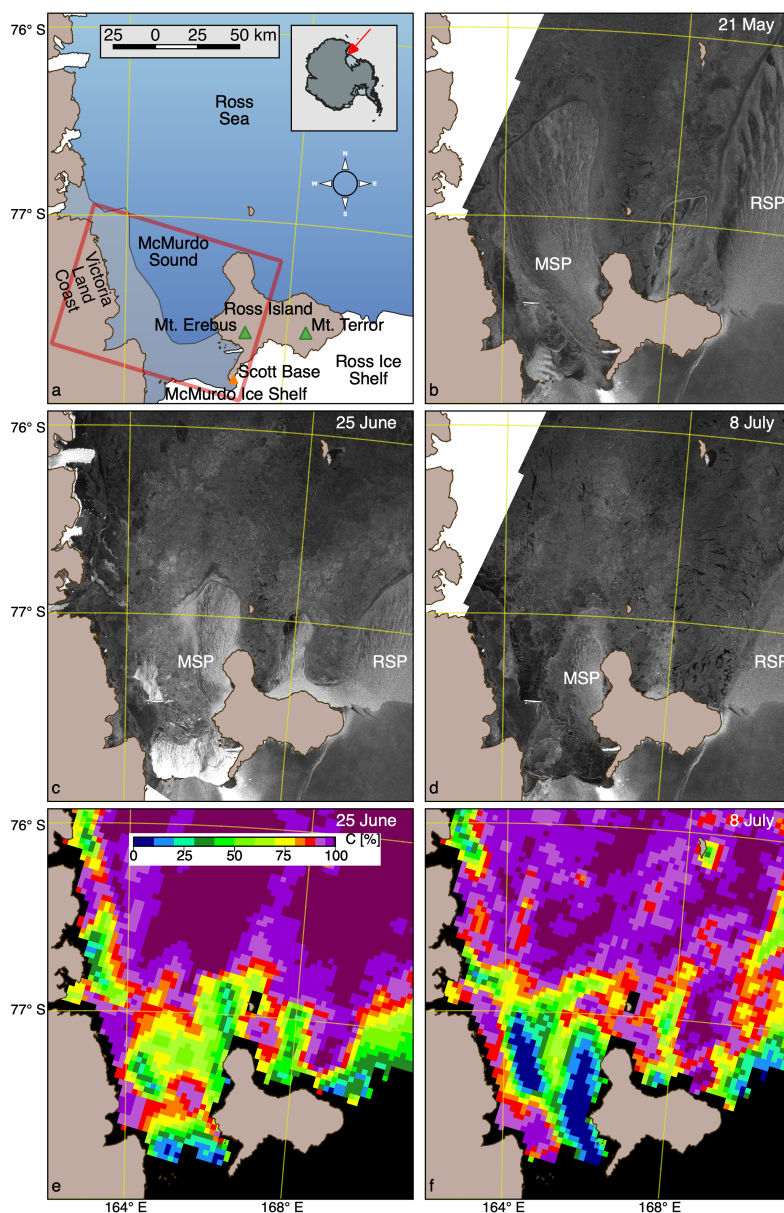


Figure 1. (a) McMurdo Sound study region, inset shows location in the Western Ross Sea, Antarctica. The red box indicates the area from which the sea ice fractions were calculated. The grey shaded area indicates fast ice extent from the middle of June 2014 from Fraser et al. (2020). (b) Sentinel-1 SAR image from 21 May, (c) 25 June and (d) 8 July. (e) Sea ice concentrations from 25 June and (f) 8 July from the ARTIST Sea Ice (ASI) algorithm (Spreen et al., 2008).

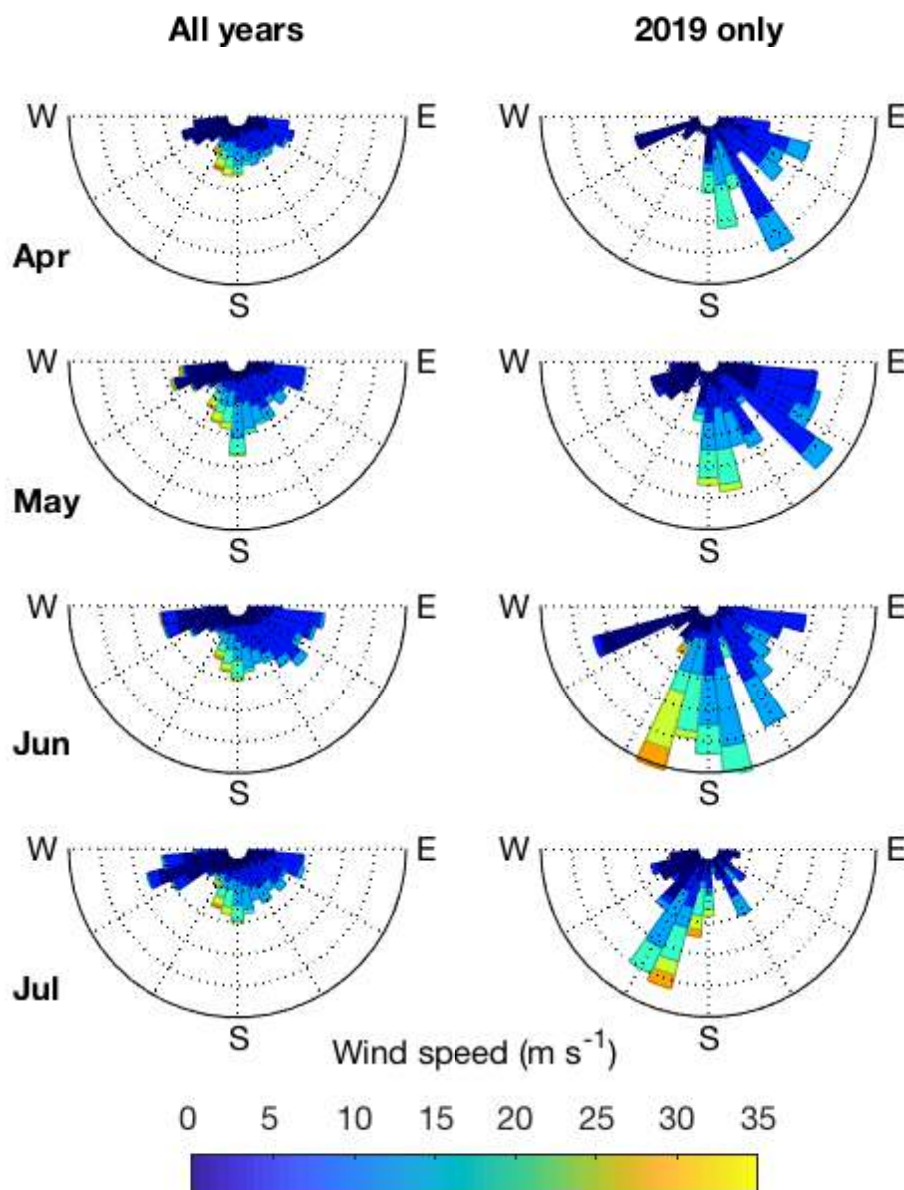


Figure 2. Wind roses showing southerly winds, as recorded at the Scott Base weather station for the months of April – July 2019. The left column is from the period 1998 – 2018 and the right column is from 2019. The maximum frequency shown on these plots is 3 %, with each circle representing an increment of 0.6 %.

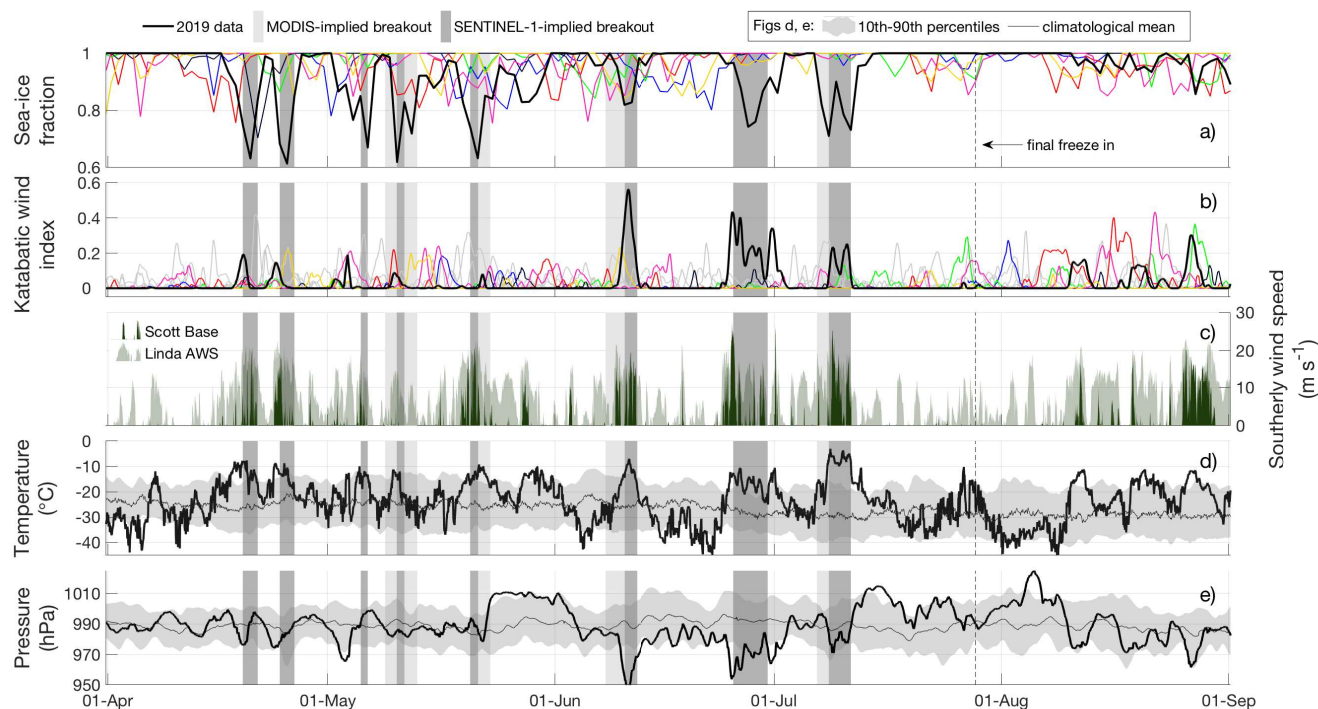


Figure 3. a) Sea ice fractional cover within the red bounding box shown in Fig. 1.a for years 2013 – 2019; Bold black: 2019, coloured lines: 2013 – 2018. b) Katabatic Wind Index (KWI) constructed from temperature and pressure anomalies for years 2002 – 2019; Bold black and coloured lines as for a), grey: years for which sea ice fraction data are not available (2002 – 2012). c) Southerly wind data from the Scott Base weather station, and Linda AWS (78.382 °S, 168.456 °E) (Lazzara et al., 2012). d–e) Air temperature and mean sea level pressure, respectively. The 10th – 90th percentiles and climatological mean include data from 1996 – 2018. Percentiles have been smoothed using a 24-hour window. Vertical shading throughout all subplots identify time periods where satellite products indicate break-out events (see Section 2.1).